
ADESSE: ADVICE EXPLANATIONS IN COMPLEX REPEATED DECISION-MAKING ENVIRONMENTS *

Sören Schleibaum

Clausthal University of Technology
soeren.schleibaum@tu-clausthal.de

Lu Feng

University of Virginia
lu.feng@virginia.edu

Sarit Kraus

Bar-Ilan University
sarit@cs.biu.ac.il

Jörg P. Müller

Clausthal University of Technology
joerg.mueller@tu-clausthal.de

ABSTRACT

In the evolving landscape of human-centered AI, fostering a synergistic relationship between humans and AI agents in decision-making processes stands as a paramount challenge. This work considers a problem setup where an intelligent agent comprising a neural network-based prediction component and a deep reinforcement learning component provides advice to a human decision-maker in complex repeated decision-making environments. Whether the human decision-maker would follow the agent's advice depends on their beliefs and trust in the agent and on their understanding of the advice itself. To this end, we developed an approach named ADESSE to generate explanations about the adviser agent to improve human trust and decision-making. Computational experiments on a range of environments with varying model sizes demonstrate the applicability and scalability of ADESSE. Furthermore, an interactive game-based user study shows that participants were significantly more satisfied, achieved a higher reward in the game, and took less time to select an action when presented with explanations generated by ADESSE. These findings illuminate the critical role of tailored, human-centered explanations in AI-assisted decision-making.

1 Introduction

Making complex decisions repeatedly in a dynamic environment is very challenging for humans. An intelligent agent can support human decision-making by providing advice. We consider an adviser agent consisting of two components as shown in Figure 1. At each step, the agent first makes some predictions about the future, and then computes advice based on the prediction and the current state using deep reinforcement learning (DRL). Such adviser agents can and are being used in many real-world applications: For example, providing advice to police officers scheduled through place-based predictive policing [1], providing advice to taxi drivers based on the prediction of future pick-up requests from passengers [2], or providing advice to firefighters based on the prediction of wildfire risk [3].

Studies have found that the degree to which humans follow an intelligent agent's advice depends on their beliefs about the agent's performance on a given task [4], and that providing explanations improves humans' acceptance and trust in the agent's advice [5, 6]. Hence, this work aims at generating explanations about the adviser agent to improve human's trust and decision-making.

Existing methods for explaining AI-based systems mostly treat the entire system as a black-box model; the generated explanations could be in different output formats (e.g., numerical, textual, visual), but each method usually only focuses on one type of explanations [7, 8, 9]. For example, there are several methods (e.g., [10, 11]) explaining the feature importance of prediction; and there is a growing body of research on explainable reinforcement learning [12, 13, 14, 15]. Nevertheless, to the best of our knowledge, none of the prior works generates explanations for both prediction and DRL.

**Citation:* This preprint has been accepted for publication at IJCAI'24. The final version is available at 10.24963/ijcai.2024/875

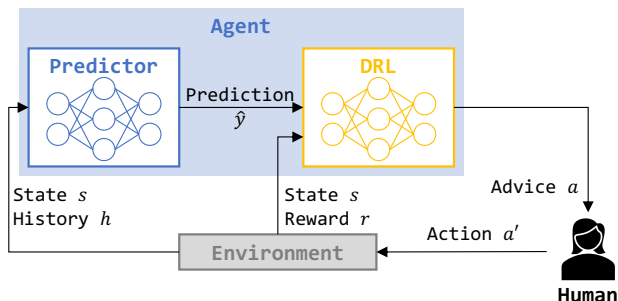


Figure 1: An agent consisting of two components provides advice to a human decision-maker.

In this work, we present a novel approach named ADESSE (ADvice EXplanations in complex repeated deciSion-making Environments)². ADESSE peeks inside the black-box model of an adviser agent, leveraging the agent’s two-component structure to generate explanations with both textual and visual information. Specifically, an explanation generated by ADESSE includes three key elements: (1) a short list of top-ranked input features that contribute the most to the agent’s prediction; (2) a heatmap visualizing domain-specific indices summarizing the DRL input features; and (3) arrows in various shades of gray overlaying the heatmap to illustrate a trained DRL policy with state importance.

A key innovation of ADESSE is to generate informative explanations that capture multiple aspects of the adviser agent, from the prediction input to the DRL input to the trained DRL policy. Furthermore, ADESSE reduces the explanation size via selecting top-ranked input features of the prediction and using domain-specific indices to succinctly explain DRL input features.

We adopt LIME [10], a popular method for explaining black-box models, as a baseline for comparison. LIME generates explanations represented as (multiple) saliency maps visualizing each input feature’s influence on the agent’s advice, which can be overwhelming when there is a large number of input features. We hypothesize that explanations generated by ADESSE can be more effective in assisting human decision-making than the baseline.

Computational experiments demonstrate that ADESSE can be successfully applied to a range of environments and scales over varying model sizes. In all cases, ADESSE generates smaller explanations using less time, compared with LIME.

Additionally, we conduct an interactive game-based user study to evaluate the effectiveness of generated explanations. Study results show that participants were significantly more satisfied, achieved a higher reward in the game, and took less time to select an action when presented with explanations generated by ADESSE rather than the baseline.

2 Related Work

2.1 Position within the XAI Literature

The research field of *explainable artificial intelligence* (XAI) has been growing rapidly in recent years, attracting increasing attention [7, 8, 9, 16, 17]. Here, we position this work based on a taxonomy of XAI methods described in [9].

First, depending on the stage when explanations are generated, there are *ante-hoc* and *post-hoc* methods. This work belongs to the latter since ADESSE generates explanations after the agent has been trained.

Second, there are *model-specific* and *model-agnostic* methods. ADESSE is agnostic to the underlying machine learning techniques for prediction and advice computation.

Third, the scope of explanations can be *global* or *local*. An explanation generated by ADESSE consists of three key elements, in which the first element (i.e., a list of top-ranked features for the prediction at a grid cell) is local and the other two elements (i.e., domain-specific indices and arrows for visualizing a DRL policy) are global.

Moreover, XAI methods generate explanations in diverse output formats, including numerical, textual, visual, rules, models, etc. ADESSE generates explanations displayed visually as a heatmap together with textual information about a short list of top-ranked features.

²ADESSE means “to aid” in Latin.

Last but not least, the lack of user studies is a major limitation across many existing XAI works, as pointed out in several survey papers [13, 18, 19]. This work overcomes this limitation by adopting an interactive game-based user study for evaluation.

At first glance, the motivating examples described in the next section seem similar to the task of goal recognition. However, in contrast to goal recognition (see [20]), we have time-dependent targets and do not learn a probability distribution over goals. Consequently, we cannot base our work on those explaining goal recognition, e.g. [21].

2.2 Feature Importance

Many XAI methods explain black-box models via computing *feature importance* (e.g., how much a feature contributes to a prediction). *Local Interpretable Model-agnostic Explanations* (LIME) [10] and *SHapley Additive exPlanations* (SHAP) [11] are two of the most popular methods in this category.

LIME focuses on training local surrogate models to explain individual predictions. This method works by first generating a new dataset comprising perturbed samples and the corresponding predictions of the black box model, and then using this new dataset to train an interpretable surrogate model that is weighted by the proximity of the sampled instances to the instance of interest. The learned surrogate model can provide a good approximation of local predictions, but does not necessarily guarantee global accuracy.

On the other hand, SHAP computes Shapley values of features (i.e., the average marginal contribution of a feature value across all possible coalitions) by considering all possible predictions for an instance using all possible combinations of inputs. Because of this exhaustive analysis, SHAP can take much longer computation time than LIME. The authors of [11] show that SHAP can guarantee properties such as accuracy and consistency, while LIME is a subset of SHAP but lacks these properties.

2.3 Explainable Reinforcement Learning

Explainable reinforcement learning (XRL) has emerged as a sub-field of XAI with a growing body of research [12, 13, 14, 15]. Existing XRL methods can be distinguished by the scope of explanations. Some methods provide explanations about policy-level behaviors, while others explain specific, local decisions (e.g., “Why does the agent select this but not that action in a state?”). Although this work seeks to explain the agent’s advice for the current state, we do not restrict to local explanations. The proposed ADESSE approach provides a policy-level explanation that shows what the agent’s advice would be in different states with varying features, which can help the human decision-maker better understand the agent’s behavior, rather than providing a local explanation about the advised action only. Thus, ADESSE intrinsically aims at increasing the humans’ trust in the adviser agent (cf. [6]).

Various types of policy-level explanations have been developed in prior works. For example, a video highlighting the agent’s trajectories with important states is proposed in [22]; such trajectory summaries are augmented with saliency maps in [23]. Abstracted policy graphs (i.e., Markov chains of abstract states) are introduced in [24] for summarizing RL policies. A chart illustrating the agent coordination and task ordering is used for policy summarization of multi-agent RL in [25]. Additionally, policy-level contrastive explanations (e.g., “Why does the agent follow this but not that policy?”) have been considered in [26, 27, 28].

To the best of our knowledge, however, none of the existing XRL methods uses a heatmap of domain-specific indices to summarize DRL input features as in ADESSE. Furthermore, we overlay the heatmap with arrows visualizing (advised) optimal actions based on a trained RL policy and annotate these arrows with different shades of gray to indicate the importance degrees of states. We follow the notion of *state importance* originally proposed in [29], which was adopted in [22] for summarizing the RL agent’s behavior in a selected set of important states. By contrast, our explanation shows the agent’s action in every state but highlights importance states with darker arrows.

2.4 Explainable Recommendations

There is a related line of work on *explainable recommendations* [30, 31, 32], which refers to recommendation algorithms that not only provide recommendation results, but also explanations to clarify why such items are recommended. For example, image and text-based explanations are generated in [33] by first selecting a personalized image set that is the most relevant to a user’s interest toward a recommended item and then producing natural language explanations. User needs for explanations of recommendations are investigated in [34], where studies find that users in high-involvement domains (e.g., selecting a car to buy) focus more on explanations compared to lower-involvement domains (e.g., selecting a movie to watch).

This work seeks to explain the agent’s advice, which can be considered as a type of recommendation; and ADESSE also provides explanations with both visual and textual information. However, our problem setup is different from those recommendation algorithms, which usually do not consider repeated decision-making in complex environments.

3 Problem Setup

We consider a problem setup where an intelligent agent comprising a neural network-based prediction component and a deep reinforcement learning (DRL) component provides advice to a human decision-maker in complex repeated decision-making environments.

As illustrated in Figure 1, at each step, the agent makes some prediction \hat{y} about the future based on the current state s and historical data h , and generates an advice a based on a trained DRL policy with the input s and \hat{y} , and reward r ; the human decision-maker takes an action a' where $a' = a$ if the human follows the agent’s advice. But sometimes, an alternative action ($a' \neq a$) may be chosen if the human does not trust the agent or does not understand why the agent proposes a certain advice.

This work aims to tackle this problem by generating explanations about the adviser agent to improve the human’s trust and decision-making. We make two important assumptions as follows.

- **A1:** The agent is rational (i.e., seeking to maximize the expected discounted return) and not adversarial to the human decision-maker (i.e., no deception).
- **A2:** The environment is based on a grid representation with discrete states and actions.

3.1 Motivating Examples

The aforementioned problem setup is commonly shared by many complex repeated decision-making environments. Here we describe two motivating examples used in this work.

Taxi environment Consider a taxi moving around in a grid world. In our example scenario, we assume the grid size to be 20×20 . The taxi can stay put or move horizontally, vertically, or diagonally by up to two grid cells at each step; we assume that one step corresponds to ten minutes real time. The taxi receives a reward of 10 for dropping off a passenger and a penalty of -1 per step for driving without any passenger. In each episode, the taxi starts at a random grid cell and time and terminates by the end of a nine-hour shift (i.e., 54 steps).

At each step of an episode, the adviser agent predicts the number of pick-up requests in each grid cell for the next step, based on a rich set of features, including the number of pick-up requests of the last 40 minutes, points of interest in each cell, as well as location-independent features such as date, time, holiday, and weather. Then, the agent advises an action for the taxi based on a DRL policy trained using the number of predicted pick-up requests and available taxis in each grid cell and the received reward.

The taxi driver decides whether to follow the agent’s advice or take an alternative action, which would impact the environment’s feedback of state and reward. The above process repeats until the end of an episode.

Wildfire environment Consider an aerial vehicle (AV) flying over a forest (modeled as a grid world) aiming to extinguish a wildfire. At each step (corresponding to 2.5 minutes), the AV can choose one of three types of actions: (1) extinguish the fire in the current grid cell, (2) stay put, or (3) decide to relocate by one cell in either of the four cardinal directions. When the AV chooses the *extinguish* action in a grid cell with a high neighborhood fire ratio, the AV receives a large positive reward that is calculated based on the neighborhood fire ratio. The AV receives a penalty of -2.5 for taking the *extinguish* action in a grid cell with a low neighborhood fire ratio, and a cost of -1 per step for moving around. In each episode, the AV starts at a random grid cell and terminates after 100 steps.

At each step, the adviser agent predicts the fire risk (i.e., the probability of fire occurrences) in each grid cell, based on features including each grid cell’s forest fuel level and burning status. Then, the agent advises an action for the AV based on a DRL policy trained using the fire risk prediction, the current state and the received reward.

The AV operator decides whether to follow the agent’s advice, which would also affect the state of the environment. The above process repeats until an episode terminates.

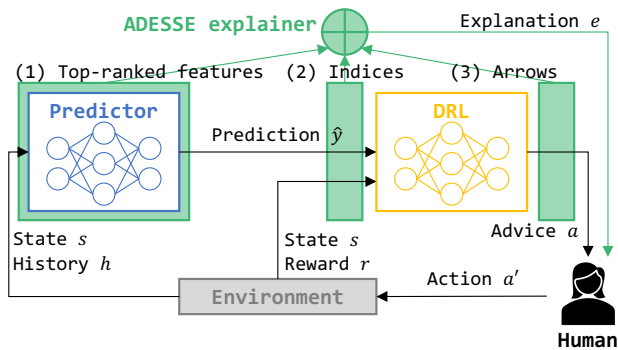


Figure 2: An explanation generated by ADESSE consists of (1) a list of top-ranked features for the prediction, (2) domain-specific indices summarizing the DRL input features, and (3) arrows visualizing the trained DRL policy.

3.2 Baseline Explanations

The baseline explainer considers a black-box model consisting of the adviser agent’s two components as a whole and explains input features’ influence on the output advice. We apply LIME [10] to check what happens to the agent’s advice when the input features are perturbed and compute an influence value for each feature. We select LIME to generate baseline explanations (cf. Subsection 3.2), because SHAP is too slow for computational experiments. SHAP yields time-out (i.e., more than two minutes) for most models used in our experiments, while LIME and the proposed ADESSE approach can generate explanations within a few seconds. The generated baseline explanations are represented as saliency maps showing how much each feature contributes to the agent’s advice.

For an example saliency map illustrating the influence of each grid cell’s current pick-up request counts on the agent’s advice see the Appendix. The baseline explanation generated at each step may include multiple saliency maps corresponding to different features. For example, there are five saliency maps generated for the taxi environment per step. We hypothesize that such a baseline explanation is overwhelming and cannot effectively assist humans with decision-making.

4 Approach

To address the limitations of baseline explanations, we propose an approach named ADESSE that leverages the problem structure and generates explanations consisting of three key elements as shown in Figure 2. First, a list of top-ranked features is selected based on their contributions to the prediction (cf. Subsection 4.1). Second, a domain-specific index function is used to summarize the DRL input features (cf. Subsection 4.2). Third, the trained DRL policy is visualized as arrows in a grid world with importance degrees (cf. Subsection 4.3). And finally, we describe how ADESSE generates an explanation integrating these elements (cf. Subsection 4.4).

4.1 Top-Ranked Features for the Prediction

We rank input features of the prediction component based on Shapley values computed via SHAP [11], which tells us the contribution of each feature to the prediction. We favor SHAP over LIME here, because identifying the top-ranked features for a few selected predictions with the smaller search space allows a fast computation time and we want the properties guaranteed by SHAP.

To reduce the explanation size, we focus on selecting a short list of top-ranked features for an individual prediction output at a time. For example, for the taxi environment, the human decision-maker may be interested to know what are the top six features contributing to the pick-up request prediction at the taxi’s current location or the advised next location. Such explanations could improve the human’s trust in the agent’s prediction component.

During a game-based user study (cf. Section 6), the human decision-maker can choose from a list of locations (e.g., grid cells labeled with A-F in Figure 3) for displaying the top-ranked features that contribute the most to the prediction in each location.

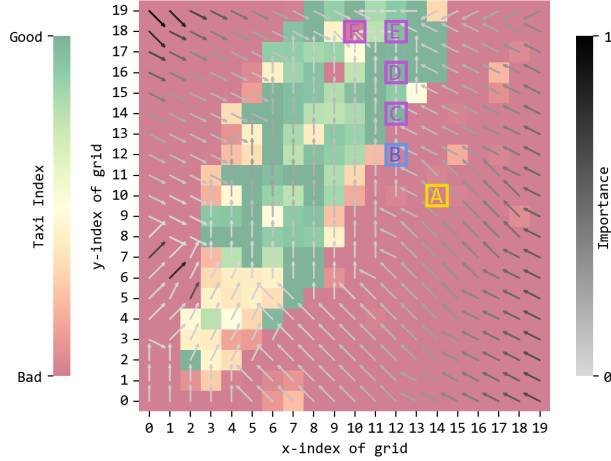


Figure 3: An example of ADESSE explanation for the taxi environment. A is the taxi’s current location and B is the advised next location, which lead to C-F in the next few steps following the trained DRL policy visualized as arrows. A list of top-ranked features would be displayed separately when the human selects one of these labelled locations.

4.2 Domain-Specific Indices

To explain the input of the agent’s DRL component, we summarize the DRL input features using a domain-specific index function, rather than showing multiple saliency maps (i.e., one for each DRL input feature) as in baseline explanations.

Taxi environment Recall from Subsection 3.1 that the DRL input features for the taxi environment include the number of predicted pick-up requests and available taxis in each grid cell. Inspired by the *demand-supply ratio*, a metric commonly used in the market for taxi services [35], we define an index function for the taxi environment as follows.

$$\phi_{\text{taxi}}(g) = \begin{cases} \eta \cdot \frac{\rho(g)}{\tau(g)} + (1 - \eta) \cdot \frac{\rho(g) \cdot |G|}{\sum_{g' \in G} \rho(g')} & \text{if } \tau(g) > 0 \\ 0 & \text{otherwise} \end{cases} \quad (1)$$

where $g \in G$ is a grid cell in the taxi grid world, $|G|$ is the total number of grid cells, and $\rho(g)$ and $\tau(g)$ are the number of predicted requests and available taxis in a grid cell g , respectively. We set $\eta = 0.75$ to balance the trade-off between the demand-supply ratio of taxi services and the ratio of predicted requests in a grid cell g compared with the average requests over the entire grid world G . Figure 3 shows an example heatmap of the obtained taxi indices where the darkest red indicates that $\phi_{\text{taxi}}(g) = 0$.

Wildfire environment For each grid cell g in the forest grid world G , the DRL input features for the wildfire environment include the predicted fire risk $\mu(g) \in [0, 1]$, the normalized forest fuel level $\theta(g) \in [0, 1]$ and the burning status $\beta(g) \in \{true, false\}$. We define an index function for the wildfire environment based on domain knowledge [36, 3] as follows.

$$\phi_{\text{fire}}(g) = \begin{cases} -\theta(g) \cdot \mu(g) & \text{if } \beta(g) = true \\ (1 - \theta(g)) \cdot (1 - \mu(g)) & \text{otherwise} \end{cases} \quad (2)$$

The intuition is that, when a grid cell has caught fire, a higher forest fuel level and higher predicted fire risk would lead to more severe fire, and hence a more negative value of the wildfire index; conversely, when a cell is not on fire, it is safer (i.e., more positive value of the wildfire index) when there is a lower forest fuel level and lower predicted fire risk. An example heatmap of the obtained wildfire indices is shown in the Appendix.

4.3 Arrows with Importance Degrees

To improve the human decision-maker’s trust in the adviser agent, we visualize the trained DRL policy for the entire grid world rather than only displaying the agent’s advice for the current grid cell.

Let $g_t \in G$ denote the current grid cell at time t . The DRL state σ_t is given by the environment state s_t (which includes g_t as a feature) and the predicted state \hat{y}_t . Let $\sigma_t[g]$ denote a DRL state that replaces g_t with a grid cell $g \in G$ but

Algorithm 1 Generating an explanation at a time step t

Input: Grid world G , current grid g_t , current state s_t , predication input x_t and output \hat{y}_t , DRL input $\sigma_t \subseteq s_t \cup \hat{y}_t$ and policy π_t

Parameter: Optional list of parameters

Output: Explanation e_t

- 1: **for all** g in a finite path starting from g_t following π_t **do**
 - 2: $F \leftarrow$ append top-ranked features $f(g) \subset x_t$
 - 3: **end for**
 - 4: **for all** $g \in G$ **do**
 - 5: Compute domain-specific indices $\phi(g)$ based on σ_t
 - 6: Compute optimal action $a(g)$
 - 7: Compute the normalized importance degree $\delta(g)$
 - 8: **end for**
 - 9: **return** $e_t = \langle F, \{\phi(g)\}_{g \in G}, \{a(g), \delta(g)\}_{g \in G} \rangle$
-

preserves all the other features of σ_t . For example, in the taxi environment, $\sigma_t[g]$ represents a state where g is an assumed location of the taxi, and the rest of DRL input features (i.e., number of predicted pick-up requests and available taxis at each grid cell) stay the same as in σ_t .

Given a trained DRL policy π_t at time t , the optimal action $a(g)$ in a grid cell g seeks to maximize the Q-value that estimates the rewards ultimately achievable by taking an action in a state.

$$a(g) = \pi_t(\sigma_t[g]) = \arg \max_{\alpha} Q(\sigma_t[g], \alpha) \quad (3)$$

where α denotes any possible action in state $\sigma_t[g]$.

Figure 3 plots the optimal action in each grid cell as an arrow overlaying the index heatmap obtained from Subsection 4.2. Moreover, we annotate these arrows with various shades of gray to represent the normalized importance degrees. We define the importance degree of each grid cell $g \in G$ following the notion of *state importance* proposed in [29]:

$$I(g) = \max_{\alpha} Q(\sigma_t[g], \alpha) - \min_{\alpha} Q(\sigma_t[g], \alpha) \quad (4)$$

Intuitively, if all actions in a state share the same Q-value, then the state is the least important for advising because it does not matter which action is chosen. We normalize importance degrees $I(g)$ over the entire grid world G and obtain:

$$\delta(g) = \frac{I(g) - \min_{g \in G} I(g)}{\max_{g \in G} I(g) - \min_{g \in G} I(g)} \quad (5)$$

such that the normalized importance degree $\delta(g) \in [0, 1]$.

4.4 Explanation Generation Algorithm

Algorithm 1 illustrates the procedure of ADESSE generating an explanation at a time step t by integrating these aforementioned elements. First, a set of locations along a finite path starting from the current grid g_t and following the trained DRL policy π_t is identified (e.g., A-F in Figure 3) and a list of top-ranked input features for the prediction in each location is selected as described in Subsection 4.1. Next, for each grid $g \in G$ in the grid world, a domain-specific index (e.g., $\phi_{\text{taxi}}(g)$ and $\phi_{\text{fire}}(g)$ introduced in Subsection 4.2) is computed to summarize the DRL input features and plotted in a heatmap. Lastly, the optimal action $a(g)$ and the normalized importance degree $\delta(g)$ for each grid $g \in G$ is computed following Subsection 4.3, which are plotted as arrows with various shades of gray overlaying the heatmap of indices. The generated explanation is returned as a heatmap as shown in Figure 3, together with separate lists of top-ranked features for the prediction.

5 Computational Experiments

We build a prototype implementation³ of ADESSE and compare its performance with the baseline explainer using LIME (cf. Subsection 3.2) via computational experiments on the taxi and wildfire environments with varying model sizes.

³<https://github.com/sorencs/ADESSE>

Environment		Explanation Size		Time (seconds)	
Domain	$ G $	Baseline	ADESSE	Baseline	ADESSE
Taxi	10×10	0.71K	0.24K	7.2	0.9
	20×20	2.81K	0.84K	10.0	1.3
	40×40	11.21K	3.24K	18.3	5.9
	80×80	44.81K	12.84K	41.2	25.5
Wildfire	10×10	0.30K	0.24K	0.9	0.2
	20×20	1.20K	0.84K	1.5	0.4
	40×40	4.80K	3.24K	2.9	0.9
	80×80	19.20K	12.84K	8.5	3.0

Table 1: Results of computational experiments.

5.1 Implementation

Taxi environment We implemented the prediction component as a feed-forward neural network consisting of five fully connected layers with 20, 128, 64, 32, and 16 neurons; and utilized the dueling double deep Q-learning [37] for the DRL component (three convolutional and three fully connected layers). The New York City Yellow Taxi dataset⁴ was used for training and validation (186 million trips taken between January 2015 and June 2016), where the GPS start and end locations of trips were mapped to grid cells in the environment.

Wildfire environment For this environment, we implemented the prediction component as a feed-forward neural network with three layers of 6, 512, and 512 neurons; as in the taxi environment, dueling double deep Q-learning [37] was used for the DRL component (three convolutional and three fully connected layers). The environment dynamics (forest fire model) was adapted from [36, 3].

Setup All experiments were run on a MacBook laptop with an Apple M1 Pro chip, 32 GB of memory, and Ventura 13.5.2 operating system.

5.2 Results

Table 1 shows the experimental results. For each model, we report the grid world size $|G|$, and compare the baseline and ADESSE in terms of the explanation size and the average time of generating an explanation per step over 10 independent runs. We draw the following key insights from the results:

- Both the baseline explainer and ADESSE can successfully generate explanations for different environments with varying model sizes.
- The size of ADESSE explanation is significantly smaller than that of the baseline explanation across all models, and the size difference increases as the grid world grows larger.
- ADESSE is generally faster than the baseline and can generate an explanation within a few seconds for all models used in the experiments.

6 Game-Based User Study

We evaluate the effectiveness of explanations generated by ADESSE via an interactive game-based user study⁵. We describe the study design in Subsection 6.1, report the results and discuss the insights in Subsection 6.2.

6.1 Study Design

Game We designed an interactive game based on the taxi environment described in Subsection 3.1. Each study participant was asked to act as a taxi driver who was incentivized to choose the optimal action in the environment at each step, in order to receive a high reward. The participants were presented with baseline explanations and with

⁴<https://www.nyc.gov/site/tlc/about/tlc-trip-record-data.page>

⁵The study was approved by institutional review board.

explanations generated by ADESSE; our goal was to find to what extent and how this influences their decisions in terms of whether or not to follow the advised actions. An example screenshot of the game user interface is shown in the Appendix.

Participants We recruited 28 participants; all of them were over the age of 18, fluent in English (since the game instructions were written in English), and did not have color blindness (which would have affected their ability to recognize the presented explanations). The average age of the participants was 28.96 years with a standard deviation of 8.27 years⁶. 39% of the participants were female and 61% male. To ensure data quality, each participant responded to three attention-check questions during the study.

Independent variables We adopted a within-subject study design where participants were asked to engage in two study trials, each of which involved playing the game for twelve steps with explanations generated by either ADESSE or by the baseline explainer using LIME. To counterbalance the ordering confound effect, one half of the participants were randomly selected to start the study trial with baseline explanations, followed by a trial with explanations generated by ADESSE; the other half of the participants took the two study trials in reversed order.

Dependent variables We recorded the average time spent to choose an action, the total reward achieved in a study trial, and the percentage of steps where the agent's advice was followed in a trial. At the end of each study trial, we also collected the participant ratings on a 5-point Likert scale (1 - strongly disagree, 5 - strongly agree) about the following statements adapted from [38] regarding *the explanation satisfaction scale*:

- The explanations help me *understand* how the agent's advice is computed.
- The explanations are *satisfying*.
- The explanations are sufficiently *detailed*.
- The explanations are sufficiently *complete*, that is, they provide me with all the needed information to make decisions.
- The explanations are *actionable*, that is, they help me know how to make decisions.
- The explanations let me know how *reliable* the agent is for decision support.
- The explanations let me know how *trustworthy* the agent is for decision support.

Procedure During the study, each participant was first briefed about the study purpose and the game instructions. Then, the participant was asked to play a study trial with one type of explanation (i.e., baseline or ADESSE) and give ratings on the explanation satisfaction scale. Next, the participant was asked to play a second trial with the other explanation type, followed by explanation satisfaction ratings. The study was wrapped up with demographic questions (e.g., age, gender). Additionally, to gain better insights into the behavior of participants, we asked a randomly selected set of participants to describe what their decision-making strategy was, and give an appraisal of how confident they were to choose a better action than the agent's advice.

Hypotheses We investigated three hypotheses stated below.

- **H1:** Explanations generated by ADESSE *lead to higher ratings on the explanation satisfaction scale* than the baseline.
- **H2:** Explanations generated by ADESSE enable the participants to *take less time to choose actions* than the baseline.
- **H3:** Explanations generated by ADESSE enable the participants to *achieve a higher total reward* than the baseline.

6.2 Study Results and Discussion

We utilized a Wilcoxon signed-rank test to evaluate H1 and used a paired t-test to evaluate H2 and H3. For all tests, we set the significance level as 0.05.

⁶Note that drivers of private transportation services such as Uber represent the demographic group from which we recruited the subjects for the study.

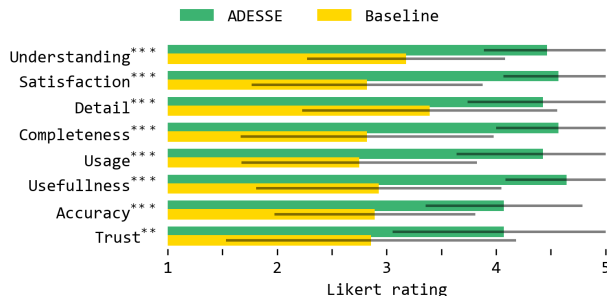


Figure 4: Mean and standard deviation of participant ratings on the explanation satisfaction scale comparing explanations generated by ADESSE (top/green) and the baseline (bottom/gold). (** for $0.001 < p \leq 0.01$ and *** for $p \leq 0.001$.)

Explanation satisfaction scale ratings As shown in Figure 4, participants ratings of explanations generated by ADESSE are higher than ratings of the baseline in all explanation satisfaction scale metrics with statistically significant differences. Thus, the data supports H1.

Time for choosing actions On average, participants took less time to choose actions when being presented with explanations generated by ADESSE ($M = 38.78$, $SD = 15.90$) compared to baseline explanations ($M = 52.82$, $SD = 27.72$). The difference is statistically significant ($t = 2.9182$, $p = 0.0070$). Thus, the data supports H2.

Total reward The participants achieved a higher average reward when being presented with explanations generated by ADESSE ($M = 98.18$, $SD = 13.18$) than baseline explanations ($M = 90.18$, $SD = 18.13$). However, the paired t-test yields ($t = -1.8216$, $p = 0.0796$) with the p value slightly higher than 0.05. Thus, the data partially supports H3.

Discussion One of the reasons that participants were more satisfied with explanations generated by ADESSE, as indicated by the higher ratings on the explanation satisfaction scale, could be due to the fact that explanations generated by ADESSE are more succinct and informative than baseline explanations (note that there are five saliency maps in each baseline explanation generated by LIME). This may also justify the reason of participants took less time to choose actions with explanations generated by ADESSE, since it requires more time to read and understand baseline explanations.

7 Conclusion

We presented ADESSE, a novel approach for generating visual and text-based explanations about an intelligent agent that provides advice to a human decision-maker in complex repeated decision-making environments. The agent consists of two deep learning-based components: one for making predictions about the future, and the other for computing advised actions with deep reinforcement learning based on the predicted future and the current state. ADESSE leverages the agent’s two-component structure and generates explanations with visual and textual information, to improve the human’s trust in the agent and thus better assist human decision-making. Results of computational experiments demonstrate the applicability and scalability of ADESSE, while an interactive game-based user study shows the effectiveness of explanations generated by ADESSE.

There are several directions to explore for possible future work. First, we will extend ADESSE to be able to deal with environments with continuous state/action space, beyond grid world environments considered in this work. For example, there has been increasing interest in using deep learning to predict future blood glucose levels of diabetes patients and then compute an advised insulin dosage based on the prediction via deep reinforcement learning [39]. Moreover, we will explore an extension to the multi-agent setting where advice is computed via multi-agent DRL.

Acknowledgements

Sören Schleibaum was supported by the Deutsche Forschungsgemeinschaft under grant 227198829/GRK1931. Lu Feng was supported by U. S. National Science Foundation under grant CCF-1942836. Sarit Kraus was supported in part by the EU Project TAILOR under grant 952215.

References

- [1] Albert Meijer and Martijn Wessels. Predictive policing: Review of benefits and drawbacks. *International Journal of Public Administration*, 42(12):1031–1039, 2019.
- [2] Nahid Parvez Farazi, Bo Zou, Tanvir Ahamed, and Limon Barua. Deep reinforcement learning in transportation research: A review. *Transportation research interdisciplinary perspectives*, 11:100425, 2021.
- [3] Kyle D Julian and Mykel J Kochenderfer. Distributed wildfire surveillance with autonomous aircraft using deep reinforcement learning. *Journal of Guidance, Control, and Dynamics*, 42(8):1768–1778, 2019.
- [4] Kailas Vodrahalli, Roxana Daneshjou, Tobias Gerstenberg, and James Zou. Do humans trust advice more if it comes from ai? an analysis of human-ai interactions. In *Proceedings of the 2022 AAAI/ACM Conference on AI, Ethics, and Society*, pages 763–777, Oxford United Kingdom, 2022. ACM.
- [5] Yunfeng Zhang, Q Vera Liao, and Rachel KE Bellamy. Effect of confidence and explanation on accuracy and trust calibration in ai-assisted decision making. In *Proceedings of the 2020 conference on fairness, accountability, and transparency*, pages 295–305, Barcelona Spain, 2020. ACM.
- [6] Donghee Shin. The effects of explainability and causability on perception, trust, and acceptance: Implications for explainable ai. *International Journal of Human-Computer Studies*, 146:102551, 2021.
- [7] Amina Adadi and Mohammed Berrada. Peeking inside the black-box: a survey on explainable artificial intelligence (xai). *IEEE access*, 6:52138–52160, 2018.
- [8] Riccardo Guidotti, Anna Monreale, Salvatore Ruggieri, Franco Turini, Fosca Giannotti, and Dino Pedreschi. A survey of methods for explaining black box models. *ACM computing surveys (CSUR)*, 51(5):1–42, 2018.
- [9] Timo Speith. A review of taxonomies of explainable artificial intelligence (xai) methods. In *Proceedings of the 2022 ACM Conference on Fairness, Accountability, and Transparency*, pages 2239–2250, New York, NY, USA, 2022. Association for Computing Machinery.
- [10] Marco Tulio Ribeiro, Sameer Singh, and Carlos Guestrin. "why should i trust you?" explaining the predictions of any classifier. In *Proceedings of the 22nd ACM SIGKDD international conference on knowledge discovery and data mining*, pages 1135–1144, New York, NY, USA, 2016. Association for Computing Machinery.
- [11] Scott M Lundberg and Su-In Lee. A unified approach to interpreting model predictions. *Advances in neural information processing systems*, 30, 2017.
- [12] George A Vouros. Explainable deep reinforcement learning: state of the art and challenges. *ACM Computing Surveys*, 55(5):1–39, 2022.
- [13] Lindsay Wells and Tomasz Bednarz. Explainable ai and reinforcement learning—a systematic review of current approaches and trends. *Frontiers in artificial intelligence*, 4:48, 2021.
- [14] Alexandre Heuillet, Fabien Couthouis, and Natalia Díaz-Rodríguez. Explainability in deep reinforcement learning. *Knowledge-Based Systems*, 214:106685, 2021.
- [15] Erika Puiutta and Eric Veith. Explainable reinforcement learning: A survey. In *International cross-domain conference for machine learning and knowledge extraction*, pages 77–95. Springer, 2020.
- [16] Waddah Saeed and Christian Omlin. Explainable ai (xai): A systematic meta-survey of current challenges and future opportunities. *Knowledge-Based Systems*, 263:110273, 2023.
- [17] Sule Anjomshoe, Amro Najjar, Davide Calvaresi, and Kary Främling. Explainable agents and robots: Results from a systematic literature review. In *18th International Conference on Autonomous Agents and Multiagent Systems (AAMAS 2019), Montreal, Canada, May 13–17, 2019*, pages 1078–1088. International Foundation for Autonomous Agents and Multiagent Systems, 2019.
- [18] Sarit Kraus, Amos Azaria, Jelena Fiosina, Maike Greve, Noam Hazon, Lutz Kolbe, Tim-Benjamin Lembecke, Jörg P. Müller, Sören Schleibaum, and Mark Vollrath. Ai for explaining decisions in multi-agent environments. In *Proceedings of the AAAI Conference on Artificial Intelligence*, volume 34, pages 13534–13538, 2020.
- [19] Tathagata Chakraborti, Sarath Sreedharan, and Subbarao Kambhampati. The emerging landscape of explainable automated planning & decision making. In *IJCAI*, pages 4803–4811, 2020.
- [20] Maayan Shvo and Sheila A McIlraith. Active goal recognition. In *Proceedings of the AAAI Conference on Artificial Intelligence*, volume 34, pages 9957–9966, 2020.
- [21] Abeer Alshehri, Tim Miller, and Mor Vered. Explainable goal recognition: a framework based on weight of evidence. In *Proceedings of the Thirty-Third International Conference on Automated Planning and Scheduling, ICAPS '23*. AAAI Press, 2023.

- [22] Dan Amir and Ofra Amir. Highlights: Summarizing agent behavior to people. In *Proceedings of the 17th International Conference on Autonomous Agents and MultiAgent Systems*, pages 1168–1176, 2018.
- [23] Tobias Huber, Katharina Weitz, Elisabeth André, and Ofra Amir. Local and global explanations of agent behavior: Integrating strategy summaries with saliency maps. *Artificial Intelligence*, 301:103571, 2021.
- [24] Nicholay Topin and Manuela Veloso. Generation of policy-level explanations for reinforcement learning. In *Proceedings of the AAAI Conference on Artificial Intelligence*, volume 33, pages 2514–2521. AAAI Press, 2019.
- [25] Kayla Boggess, Sarit Kraus, and Lu Feng. Toward policy explanations for multi-agent reinforcement learning. In *International Joint Conference on Artificial Intelligence (IJCAI)*, 2022.
- [26] Sarath Sreedharan, Utkarsh Soni, Mudit Verma, Siddharth Srivastava, and Subbarao Kambhampati. Bridging the gap: Providing post-hoc symbolic explanations for sequential decision-making problems with inscrutable representations. In *International Conference on Learning Representations*, 2022.
- [27] Mira Finkelstein, Lucy Liu, Yoav Kolumbus, David C Parkes, Jeffrey Rosenschein, Sarah Keren, et al. Explainable reinforcement learning via model transforms. In *Advances in Neural Information Processing Systems*, 2022.
- [28] Kayla Boggess, Sarit Kraus, and Lu Feng. Explainable multi-agent reinforcement learning for temporal queries. In *Proceedings of the Thirty-Second International Joint Conference on Artificial Intelligence (IJCAI)*, 2023.
- [29] Lisa Torrey and Matthew Taylor. Teaching on a budget: Agents advising agents in reinforcement learning. In *Proceedings of the 2013 international conference on Autonomous agents and multi-agent systems*, pages 1053–1060, Richland, SC, 2013. International Foundation for Autonomous Agents and Multiagent Systems.
- [30] Yongfeng Zhang, Xu Chen, et al. Explainable recommendation: A survey and new perspectives. *Foundations and Trends® in Information Retrieval*, 14(1):1–101, 2020.
- [31] Alexandra Vultureanu-Albiși and Costin Bădică. A survey on effects of adding explanations to recommender systems. *Concurrency and Computation: Practice and Experience*, 34(20):e6834, 2022.
- [32] Mohammad Naiseh, Nan Jiang, Jianbing Ma, and Raian Ali. Explainable recommendations in intelligent systems: delivery methods, modalities and risks. In *Research Challenges in Information Science: 14th International Conference, RCIS 2020, Limassol, Cyprus, September 23–25, 2020, Proceedings 14*, pages 212–228. Springer, 2020.
- [33] An Yan, Zhankui He, Jiacheng Li, Tianyang Zhang, and Julian McAuley. Personalized showcases: Generating multi-modal explanations for recommendations. In *Proceedings of the 46th International ACM SIGIR Conference on Research and Development in Information Retrieval*, pages 2251–2255, Taipei Taiwan, 2023. ACM.
- [34] Thi Ngoc Trang Tran, Alexander Felfernig, Viet Man Le, Thi Minh Ngoc Chau, and Thu Giang Mai. User needs for explanations of recommendations: In-depth analyses of the role of item domain and personal characteristics. In *Proceedings of the 31st ACM Conference on User Modeling, Adaptation and Personalization*, pages 54–65, Limassol Cyprus, 2023. ACM.
- [35] Camille Kamga, M Anil Yazici, and Abhishek Singhal. Analysis of taxi demand and supply in new york city: implications of recent taxi regulations. *Transportation Planning and Technology*, 38(6):601–625, 2015.
- [36] Ravi N Haksar and Mac Schwager. Distributed deep reinforcement learning for fighting forest fires with a network of aerial robots. In *2018 IEEE/RSJ International Conference on Intelligent Robots and Systems (IROS)*, pages 1067–1074. IEEE, 2018.
- [37] Ziyu Wang, Tom Schaul, Matteo Hessel, Hado Hasselt, Marc Lanctot, and Nando Freitas. Dueling network architectures for deep reinforcement learning. In *International conference on machine learning*, pages 1995–2003, New York, NY, USA, 2016. PMLR, JMLR.org.
- [38] Robert R Hoffman, Shane T Mueller, Gary Klein, and Jordan Litman. Metrics for explainable ai: Challenges and prospects. *arXiv preprint arXiv:1812.04608*, 2018.
- [39] Harry Emerson, Matthew Guy, and Ryan McConville. Offline reinforcement learning for safer blood glucose control in people with type 1 diabetes. *Journal of Biomedical Informatics*, 142:104376, 2023.
- [40] Marina Haliem, Ganapathy Mani, Vaneet Aggarwal, and Bharat Bhargava. A Distributed Model-Free Ride-Sharing Approach for Joint Matching, Pricing, and Dispatching Using Deep Reinforcement Learning. *IEEE Transactions on Intelligent Transportation Systems*, 22(12):7931–7942, December 2021.
- [41] Ziyu Wang, Tom Schaul, Matteo Hessel, Hado Van Hasselt, Marc Lanctot, and Nando De Freitas. Dueling Network Architectures for Deep Reinforcement Learning. In *Proceedings of the 33rd International Conference on International Conference on Machine Learning - Volume 48, ICML’16*, pages 1995–2003, New York, NY, USA, 2016. JMLR.org.

Appendices

Here, we describe details about the repositioning agent in Appendix A, the wildfire agent in Appendix B, and provide more information about the user study in Appendix C. Besides this document, the technical appendix contains (1) a file `game_log.csv` that contains the logs of each study participant playing the game with the baseline and our composed setting, and (2) the corresponding responses to the questionnaire in `questionnaire_response.csv`. Upon acceptance of the paper, the source code will be published.

A Details of the Repositioning Agent

Here, we describe the dataset, the request estimation, and the repositioning in more detail.

A.1 Dataset

In Figure 5, we visualize the distribution of the pick-up locations of the New York City Yellow Taxi dataset on a logarithmic scale. We know that this demand for requests is not the real one as it only includes those trips that took place. Nevertheless, we stick to this dataset as there is no alternative with such a large number of trips publicly available.

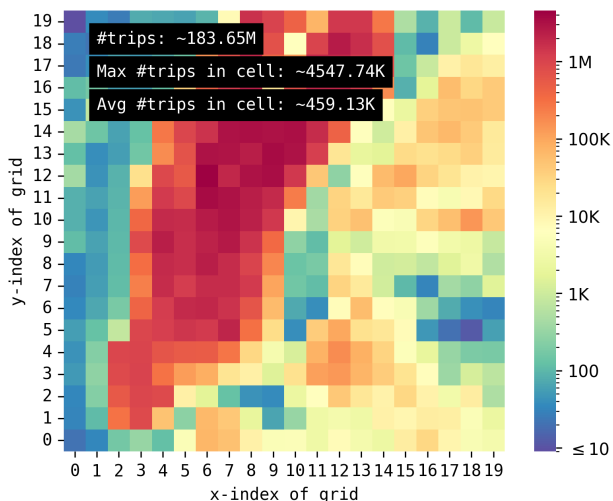


Figure 5: Distribution of the number of taxi trips in the New York City Yellow Taxi dataset in 2015 and 2016 visualized on a logarithmic scale through a 500m square grid.

A.2 Request Prediction

The request predictor consists of five fully connected layers with 20, 128, 64, 32, and 16 neurons. With a learning rate of 0.001 and 15 epochs of training, we achieve a mean absolute error of 1.26 trips per cell on the test data. As input features, we used the following: (1) x-index at location v , (2) y-index at v , (3) #requests 30 minutes ago at v , (4) #requests 20 minutes ago at v , (5) #requests 10 minutes ago at v , (6) #requests now at v , (7) #points of interests at v , (8) hour, (9) minute, (10) weekday, (11) month, (12) temperature, (13) wind, (14) humidity, (15) air pressure, (16) view, (17) whether there is snow, (18) precipitation, (19) whether there are clouds, and (20) whether the day is a public holiday.

A.3 DRL-based Repositioning

We train the repositioning agent via deep reinforcement learning. Similar to [40] and related work in taxi repositioning, we use model-free off-policy Q-learning. In particular, we use dueling double deep Q-learning as proposed by [41] with experience replay as it is closer to the state of the art in reinforcement learning than the double deep Q-learning approach used by [40]. Both networks – the policy and the target one – consist of three convolutional layers with

corresponding kernel sizes of 5, 5, and 3; the number of filters is set to 16, 32, and 64. The next layer is fully connected with $64 * 12 * 12 + 2 = 9218$ input and 1024 output neurons. Next, the dueling approach differentiates between a value and an advantage layer, which both receive the same input from the previous layers. As we do not aim to outperform other repositioning approaches but to enable explaining them, we tune the hyperparameter manually, resulting in (1) a learning rate of 0.001, (2) a gamma of 0.99, (3) an episode decay of 675 to adjust the exploration-exploitation trade-off, (4) a target network update rate of 11, (5) and a replay memory size of 15K transitions. On average, the repositioner achieves an reward of 6.85 per step in the test data.

B Details of the Wildfire Extinguishing Agent

To provide further details of the wildfire extinguishing agent, we provide details of the fire model, the fire prediction, the DRL-based wildfire extinguishing agent, and an illustration of the corresponding explanation generated by ADESSE.

B.1 Fire Model

At each time step the forest is updated, which consists of three steps: (1) When a cell is burning, its fuel is reduced by a value β . (2) For each grid cell $g \in G$ the amount of cells burning in the neighborhood (b_g) is calculated. If g is not burning and $b_g > v * \alpha$, the cell is set on fire. (3) In case the aerial vehicle dropped water to extinguish the fire on burning cells, those stop burning. We set $\alpha = 20$ and $\beta = 0.7$.

B.2 Fire Prediction

To predict the risk of fire at a location $g \in G$ the fire estimation model receives the (1) forest fuel, (2) whether or not the forest is burning, and the (3) location of the aerial vehicle. We use a feed-forward fully-connected neural network with three layers and 6, 512, and 512 nodes. As activation functions, we select Leaky ReLU and Sigmoid. The network is optimized via Adam with an initial learning rate of 0.01 through mean squared error loss. We train for up to 1000 steps, but apply early stopping with a patience of 100 steps. Further, we save the best model during training.

B.3 DRL-based Wildfire Extinguishing

The reward function used for training depends on the percentage of the fire extinguished, the number of forest cells extinguished, and the time step. We train the extinguishing agent via dueling double deep Q-learning with experience replay. Both networks – the policy and the target one – consist of three convolutional layers with corresponding kernel sizes of 3, 3, and 3; the number of filters is set to 4, 8, and 16. The fully connected layers have 68, 1024, 512, 256. Next, the dueling approach differentiates between a value and an advantage layer, which both receive the same input from the previous layers. As we do not aim to outperform other repositioning approaches but to enable explaining them, we tune the hyperparameter manually, resulting in (1) a learning rate of 0.001, (2) a gamma of 0.95, (3) an episode decay of 675, (4) a target network update rate of 256, (5) and a replay memory size of 15K transitions. After training, the agent is able to preserve 72.86% of the original forest fuel from burning.

B.4 Explanation Illustration

Figure 6 shows an example heatmap of the obtained wildfire indices, where the darkest green and red indicate that $\phi_{\text{fire}}(g) = 1$ and $\phi_{\text{fire}}(g) = -1$, respectively.

C Details of User Study

Here, we describe the profile of the study respondents, report the description of the game given to the participants, show the graphical user interface of the game, and list the questions of the questionnaire conducted in the study.

C.1 Profile of Respondents

We list the profile of the study participants in Table 2. We consider the reported sex, age, education, and country of living.

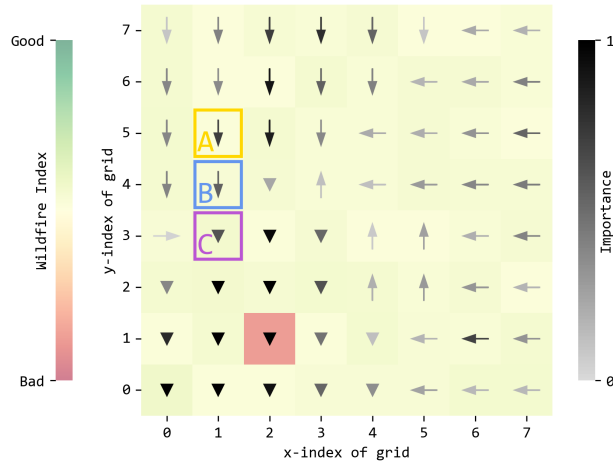


Figure 6: An example of ADESSE explanation for the wildfire environment. A is the AV’s current location and B is the advised next location, which lead to C in the next step following the trained DRL policy visualized as arrows. A list of top-ranked features would be displayed separately when the human selects one of these labelled locations.

C.2 Description of Game Given to Participants

Before each participant starts playing the game, we describe that she is a taxi driver aiming to maximize her reward. Further, we describe the following aspects: (1) the current location – yellow square – the advice – blue square – and the last location – black square – (2) that at each step a movement of up to two cells or staying at the current location is possible via the action buttons, (3) the reward function, (4) the available information fields like the accumulated reward, (5) the usage of the webpage (e.g., minimizing/maximizing of graphics and description pane) and (6) the description of the explanation configuration.

C.3 GUI of Game

In Figure 7, we show the graphical user interface of the game used in our study with our composed explanation; in Figure 8, we show the corresponding counterpart for the baseline explanation.

C.4 Questions

Here, we list the questions, the participants answered during the game-based user study.

Step 1 - Introduction to the study and the game.

- Does the blue or the yellow square represent the location of the taxi? Queried via a multiple choice question.
- Does the blue or the yellow square represent the location of the advice? Queried via a multiple choice question.
- When not limited by the city borders, can you move up to two or four cells in each direction? Queried via a multiple choice question.
- Is the goal of the game to minimize or maximize the reward? Queried via a multiple choice question.

Step 3/5 - Questions related to the subjective usage of the advice.

- How much did you follow the given advices (marked with blue)? Queried on a 5-point Likert scale.
- In case you didn’t follow the advices all the time: How confident are you, that you chose better than the given advices? Queried on a 5-point Likert scale.
- Please explain your strategy. Queried via an open text field.

Step 6 - Questions related to the explanation satisfaction scale. The corresponding questions were already described in Section 6.

Question	Answer	Overall ($n = 28$)	
		n	%
Sex	Female	11	39
	Male	17	61
	No gender	-	-
Age	No answer	-	-
	< 21	3	11
	21 to 30	17	61
	31 to 40	5	18
	41 to 50	1	4
	51 to 60	-	-
	> 60	1	4
	No answer	1	4
Education	No training yet	-	-
	Secondary school	1	4
	High school diploma	3	11
	Vocational training	2	7
	Bachelor degree	8	29
	Master degree	11	39
	Doctorates	3	11
	Other	-	-
	No answer	-	-
Country	Germany	18	64
	Israel	6	21
	United States	3	11
	Finland	1	4
	No answer	-	-

Table 2: Profile of respondents

Step 7 - Demographic questions

- How old are you?
- Which gender do you feel you belong to?
- What is currently your highest level of education?
- Which country do you live in?

Taxi Index

The Taxi Index combines the #taxis and the estimated #requests in one grid cell. It is calculated via two things: (1) The ratio between the estimated #requests and the #taxis as well as (2) the ratio between the estimated #requests and the mean #requests to include how much is going on in a cell.

Arrows

The arrows show the most promising advice from the repositioners perspective for each possible location in the grid. The darker the arrow, the more important is taking the action at that location.

Table

As the #request per cell is not known in the next 10 minutes, it is estimated via a model. The features influencing the estimation the most, are shown in the table.

Current taxi location, advice, upcoming locations

The current location is marked with a yellow rectangle, the advice with a blue one, and the ones after that with purple ones.

Taxi Repositioning Game

A/Taxi location: [14,10] Last reward: 0 Acc. reward: 0 Remaining steps: 12

Explanation of request estimation model via most important features for the selected location

Feature	Value
0 x-index	14
1 #requests now	0.5
2 #requests 30 minutes ago	0.2
3 #requests 10 minutes ago	0.1
4 y-index	10
5 #requests 20 minutes ago	0.3

Please select one of the actions by clicking on the corresponding button!

-2,2	-1,2	0,2	1,2	2,2
-2,1	-1,1	0,1	1,1	2,1
-2,0	-1,0	0,0	1,0	2,0
-2,-1	-1,-1	0,-1	1,-1	2,-1
-2,-2	-1,-2	0,-2	1,-2	2,-2

The blue button is the advice; the yellow your current location.

The button '-1,0' refers to moving one cell to the left or -1 steps on the x-axis and 0 steps on the y-axis.

Figure 7: An example screenshot of the game user interface where a participant is presented with an explanation generated by ADESSE (top of the figure) and asked to select an action (bottom of the figure). The taxi’s current location is shown in yellow and the agent’s advice is shown in blue. The left panel reminds the participant about the game instructions.

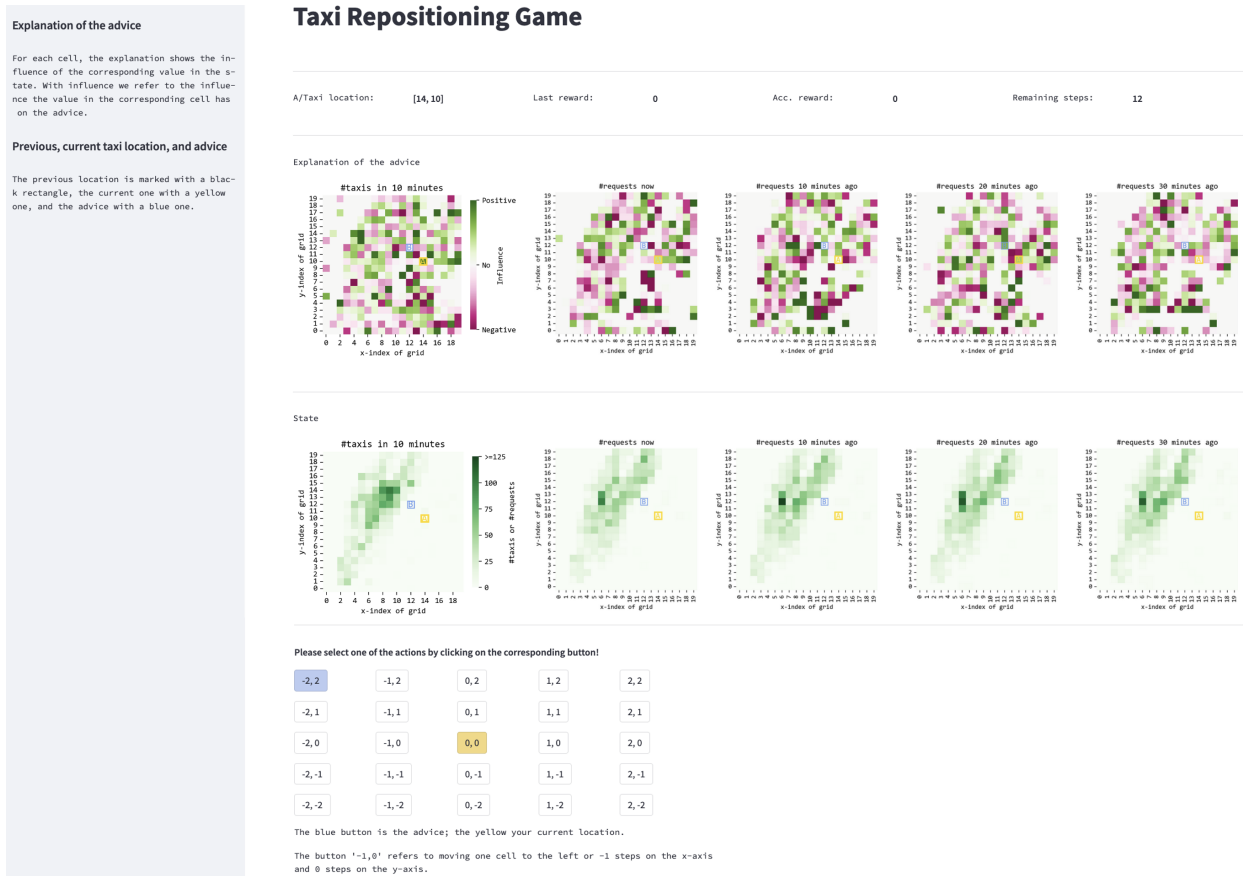


Figure 8: An example screenshot of the game user interface where a participant is presented with an explanation generated by the baseline (top of the figure) and asked to select an action (bottom of the figure). The taxi's current location is shown in yellow and the agent's advice is shown in blue. The left panel reminds the participant about the game instructions.